J Electr Eng Technol Vol. 9, No. 2: 471-477, 2014
http://dx.doi.org/10.5370/JEET.2014.9.2.471

ISSN(Print) 1975-0102
ISSN(Online) 2093-7423

Optimal Design of a Novel Permanent Magnetic Actuator using Evolutionary Strategy Algorithm and Kriging Meta-model

Seung-Ki Hong*, Jong-Suk Ro† and Hyun-Kyo Jung**

Abstract – The novel permanent magnetic actuator (PMA) and its optimal design method were proposed in this paper. The proposed PMA is referred to as the separated permanent magnetic actuator (SPMA) and significantly superior in terms of its cost and performance level over a conventional PMA. The proposed optimal design method uses the evolutionary strategy algorithm (ESA), the kriging meta-model (KMM), and the multi-step optimization. The KMM can compensate the slow convergence of the ESA. The proposed multi-step optimization process, which separates the independent variables, can decrease time and increase the reliability for the optimal design result. Briefly, the optimization time and the poor reliability of the optimum are mitigated by the proposed optimization method.

Keywords: Actuator, Circuit breaker, Evolutionary strategy, Finite element method, Kriging, Optimal design

1. Introduction

Permanent magnetic actuator (PMA) has many advantages, such as its short operation time, compact structure, high reliability, high repeatability, and low maintenance costs [1-8]. Hence, the PMA has received much attention lately for the application of a circuit breaker [1-4, 9]. Many researchers have been conducted the research on the PMA as reported in [1, 2, 5-7, 10-17] for several decades. The PMA requires a rare earth permanent magnet for high efficiency. However, the cost of a rare earth permanent magnet is steadily increasing at present, which accounts for a considerable part of the total cost of a PMA [4]. To solve this problem, we proposed a novel PMA and its optimal design method.

The proposed PMA, termed as a separated permanent magnetic actuator (SPMA), uses less permanent magnet than the existing PMA. An optimal design method using an evolutionary strategy algorithm (ESA), a kriging meta-model (KMM), and the multi-step optimization is proposed in this paper because the trial-and-error process for the design of the SPMA increases the time needed as well as the cost while introducing the reliability problem which is whether the designed result is an optimum or not.

The ESA experiences the problem of slow convergence to the global optimum [18]. To address this problem, the KMM, which is known as an effective method for the approximation of complex and nonlinear functions [19], was combined with the ESA. Hence, an effective search of the global optimum is possible while decreasing the optimization time and increasing the reliability. Furthermore, we proposed the multi-step optimal design method, which optimizes the independent variables step-by-step, because if all of the variables are optimized at once, time and reliability problems can be occurred.

† Corresponding Author: Brain Korea 21 Information Technology, School of Electrical Engineering, Seoul National University, Kwanak-gu, Seoul, Korea. (jongsukro@naver.com)
* LSIS.Co.Ltd, KyongKi-Do, Korea. (skhonga@LSIS.BIZ)
** Dept. of Electrical and Computer Engineering, Seoul National University, Korea. (hkjung@snu.ac.kr)
Received: January 3, 2013; Accepted: August 7, 2013

2. Structure and Working Principle of the SPMA

Fig. 1 shows the comparison between the conventional PMA and the proposed SPMA. If the mover is located at the top, it is in a closed state. If the mover is located at the bottom, it is in an open state. The PMA and SPMA can maintain a closed state or an open state only using the permanent magnet without any electrical power consumptions. When the closing or opening coil is excited by current, a movable electrode connected to the mover by a shaft moves and the circuit is opened or closed.

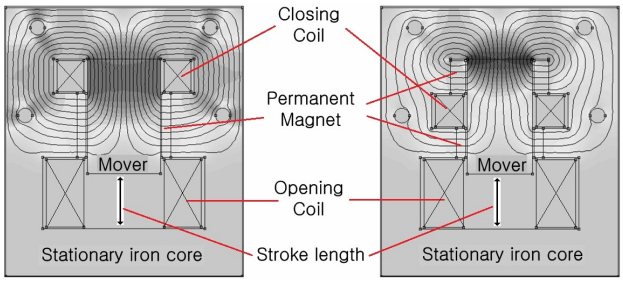

(a) PMA (b) SPMA

Fig. 1. Comparison of the calculated magnetic flux density of the closed state between the PMA and the SPMA using same amount of permanent magnets

As demonstrated in Fig. 2 (a), the SPMA maintains the closed state by using the upper and the lower permanent magnets. When the opening coil is excited as described in Fig. 2 (b), the mover starts to move. As presented in Fig. 2 (c), after the mover arrives to the opening position, the opening coil is turned off and the open state can be maintained by using only the lower permanent magnet.

When the closing coil is excited as shown in Fig. 3 (b), the mover starts the motion and then arrives to the closing position as elucidated in Fig.3 (c). After the mover arrives to the closing position, the closing coil is turned off and the closed state can be maintained by using both the upper and the lower permanent magnets without any electrical power consumption.

The holding force acts as a load to the actuator. Hence, a minimal holding force is essential. A larger value of the holding force is required for the closed state as compared to the open state. However, the conventional PMA cannot generate a different value of the holding force in the open state and the closed state [20, 21]. Moreover, the efficiency for the generation of the holding force is low because permanent magnet are located symmetrically only in the middle of the actuator. To address these problems with the PMA, we propose the novel. The opening holding force of the SPMA can be controlled independently by controlling the ratio between the upper magnet and the middle magnet. The efficiency of the SPMA is higher than the PMA with the following reasons: the magnetic flux of the PMA is concentrated in the mover, but the high magnetic flux area of the SPMA is in the air gap; the magnetic flux path of the SPMA is shorter than that of the PMA. Hence, the size and the cost of the coil, the mover, and the capacitor for the SPMA can be reduced significantly.

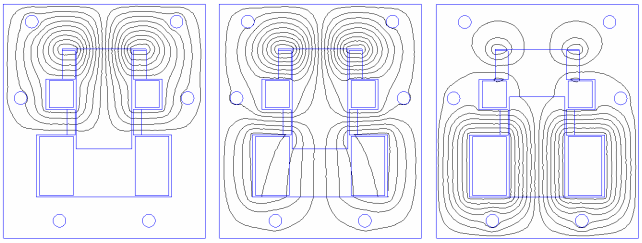

(a) (b) (c)

Fig. 2. Calculated result by using FEM for the opening of the SPMA: (a) Closed state; (b) Excitation of the opening coil; (c) After finishing the opening operation, the open state is maintained by the lower permanent magnet.

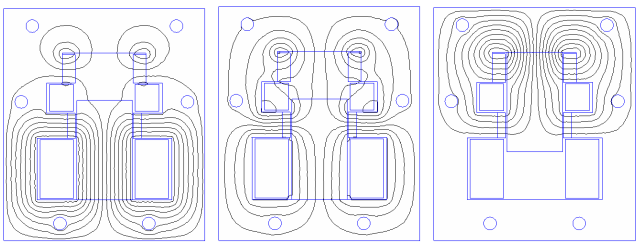

(a) (b) (c)

Fig. 3. Calculated result by using FEM for the closing of the SPMA: (a) Open state; (b) Excitation of the closing coil; (c) After finishing closing operation, the closed state is maintained by both the lower and the upper permanent magnet.

3. Analysis of the SPMA

For the analysis of the SPMA, we developed an analysis tool, which is named as SNU_SPMA. The analysis method of the SNU_SPMA is as follows.

Fig. 4 shows the equivalent circuit of the SPMA, where C is the capacitance of the capacitor, V_c is the voltage at the capacitor, T_r is the switching controller, I is the current of the coil, R_{coil} is the resistance of the coil, L is the inductance of the coil, *Diode* is the Fly-wheel diode [22].

Using the equivalent circuit and time difference method(TDM), the voltage equation and the change in the current at the n_{th} time step, dI^n, are governed respectively by: (1) and (2) while the mover is in a standstill at early in an operating stage; (3) and (4) while the mover in a motion; (6) and (7) after the mover arrived at the target position, in which L_i^n is the transformer electro-motive force (TEMF), L_x^n is the motional electro-motive force (MEMF), and V is the external input voltage with a zero value because the controller cuts off the power after the mover arrived at the target position.

$$V_c^n = (I^{n-1} + dI^n)R_{coil} + L_i^{n-1}\frac{dI^n}{dt} \tag{1}$$

$$dI^n = \frac{dt(V_c^n - I^{n-1}R_{coil})}{R_{coil}dt + L_i^{n-1}} \tag{2}$$

$$V_c^n = (I^{n-1} + dI^n)R_{coil} + L_i^{n-1}\frac{dI^n}{dt} + L_x^{n-1}\frac{dx^n}{dt} \tag{3}$$

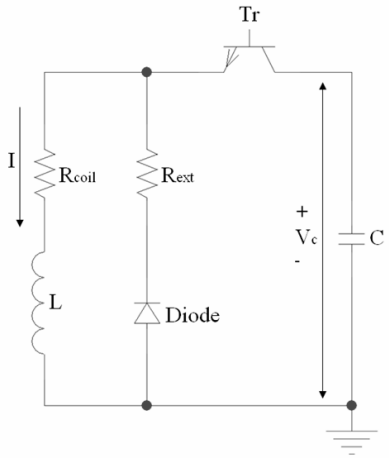

Fig. 4. The equivalent circuit of the SPMA

$$dI^n = \frac{dt(V_c^n - I^{n-1}R_{coil}) - L_x^{n-1}dx^n}{R_{coil}dt + L_i^{n-1}} \tag{4}$$

$$V = (I^{n-1} + dI^n)(R_{coil} + R_{ext}) + L_i^{n-1}\frac{dI^n}{dt} \tag{5}$$

$$dI^n = \frac{dt\left\{V - I^{n-1}(R_{coil} + R_{ext})\right\}}{dt(R_{coil} + R_{ext}) + L_i^{n-1}} \tag{6}$$

The capacitor voltage will drop, as shown by (7), until the switch controller cuts off the capacitor voltage.

$$V_c^n = V_c^{n-1} - \frac{1}{C}I^n dt \tag{7}$$

The equation of motion for the SPMA, the velocity of the mover $\vec{v}^n$ and the displacement of a mover $\vec{x}^n$ can be induced by (8, 9), and (10), respectively, where m is the mass of the mover, $\vec{g}$ is the acceleration of gravity, $\vec{F}_{mag}$ is the magnetic force acting on the mover, $\vec{F}_{spring}$ is the spring load, and $\vec{F}_{fric}$ represents the frictional force. The magnetic force $\vec{F}_{mag}$ is calculated by the magneto-static field analysis.

$$m\left(\frac{d^2\vec{x}^n}{d^2t} + \vec{g}\right) = m\left(\frac{d\vec{v}^n}{dt} + \vec{g}\right) = \vec{F}_{mag}^n + \vec{F}_{spring}^n + \vec{F}_{fric}^n \tag{8}$$

$$\vec{v}^n = \vec{v}^{n-1} + d\vec{v}^n = \vec{v}^{n-1} + \left(\frac{\vec{F}_{mag}^n + \vec{F}_{spring}^n + \vec{F}_{fric}^n - m\vec{g}}{m}\right)dt \tag{9}$$

$$\vec{x}^n = \vec{x}^{n-1} + d\vec{x}^n = \vec{x}^{n-1} + \vec{v}^n dt$$

$$= \vec{x}^{n-1} + \vec{v}^{n-1}dt + \frac{1}{2}\left(\frac{\vec{F}_{mag}^n + \vec{F}_{spring}^n + \vec{F}_{fric}^n - m\vec{g}}{m}\right)dt^2 \tag{10}$$

4. Verification of the Analysis Method

The proposed SPMA was prototyped for a 17.5(kV), 40(kA) VCB in this research. The analysis data and the experimental values are shown in Figs. 5 and Fig. 6.

In experimental data of Figs. 5 and Fig. 6, the inclination of the displacement is changed and the oscillation is occurred from a specific point, 12mm. This point is related to the compressive spring, which is installed for the stable contact of the movable electrode with a fixed electrode and for the aid of the opening operation by using the compressive force of the spring. In case of the opening operation, the oscillation starts at 12mm because the compressive spring is fully stretched at this point and the opening velocity is decreased from that point. As shown in calculated data, the change of the inclination of the displacement is taken into account in the analysis by considering the stiffness of the compressive spring. However, the oscillation could not be considered in the analysis because the oscillation is a nonlinear vibration occurred by an instantaneous change of applied force. In

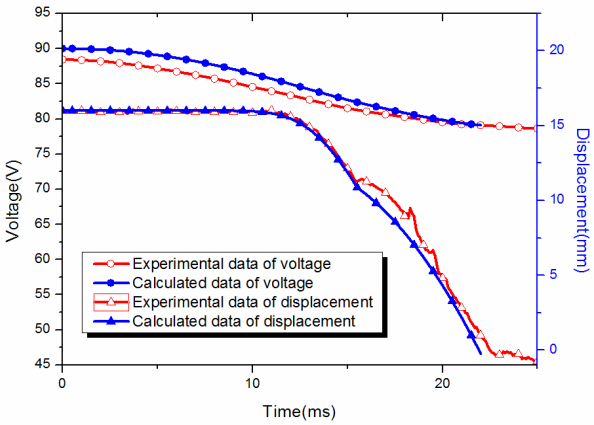

Fig. 5. The displacement of the movable electrode and the voltage of the opening capacitor during the opening operation of the verification model

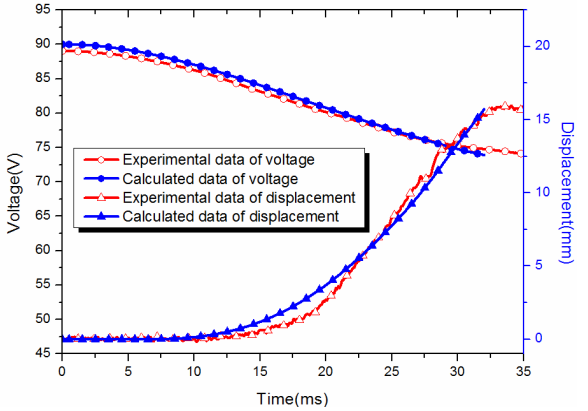

Fig. 6. The displacement of the movable electrode and the voltage of the closing capacitor during the closing operation of the verification model

case of the closing operation, similar oscillating pattern is also demonstrated because of the spring effect as the case of the opening operation.

The analysis data show good agreement with the experimental values such that the correctness of the proposed analysis method is confirmed. The minute difference between the experimental data and the calculated results shown in Figs. 5 and Fig. 6 is induced from the nonlinearity of the material.

5. Optimal Design of the SPMA

5.1 ESA combined with the KMM

The KMM creates a surrogate model, which is similar to the actual function, using data calculated through the ESA. The predicted optimum result using the KMM can be served as a candidate for the next generation of the ESA. The ESA is a stochastic algorithm. Although, the ESA can

search for a solution over a large area, the convergence to the optimum result is slow. Hence, by combining the KMM and the ESA, the global optimum can be found and the optimization time can be reduced while maintaining the high reliability.

The optimal design method is proposed for the SPMA using the ESA and the KMM via the steps shown below.

Step.0. Generation of the initial population: n individuals are generated with same grid in the problem region.

Step.1. Generation of the parent set: among the population with n individuals, μ number of elite solutions are selected as members of the parent set. In this research, μ equals to one due to the use of (1+1) ESA [23]. The remaining values are used for the surrogate model using the KMM.

Step.2. Generation of children: calculate the fitness of each solution and produce λ number of new children within the evolution range, where λ equals to one [23-25].

Step.3. Annealing: if the elite solution improves compared to the prior generation, the evolution range will be increased through division with the annealing factor to prevent convergence to the local optimum, where the annealing factor is set to 0.85 empirically. If the elite solution does not improve, the evolution range will be decreased through the multiplication with the annealing factor [23].

Step.4. Shaking: the shaking step is the generation of a random solution within the search area for diversity of the solution. In a general ESA, the frequency of shaking depends on the convergence ratio. If the degree of convergence is increased, the frequency of shaking is increased [23-25]. In the ESA combined with the KMM, the shaking number grows as the iteration is increased to improve the overall accuracy of the surrogate model and to prevent falling into the local optimum.

Step.5. Reshaping: the surrogate model, the KMM, will be updated using the calculated data during the optimization step and will converge to the actual function by the reshaping process.

Step.6. Convergence check: if a solution superior to the current elite solution is found in the reshaped surrogate model, the elite solution will be changed to the superior solution and the process will repeat steps 1 through 6 until the evolution range is under a specific value, which means the solution is converged [23].

5.2 Verification of the proposed optimization algorithm

The proposed algorithm, which is the ESA combined with the KMM, is verified through the mathematical test function (11). As demonstrated in Fig. 7, the proposed algorithm can reconstruct the function within 1% error from the real test function through 208 iterations, where

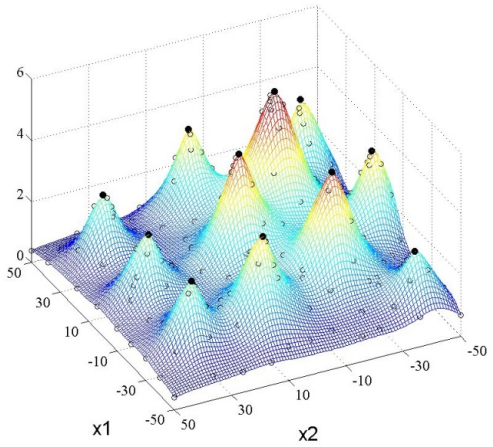

Fig. 7. Optimization result of the test function by using the proposed algorithm, which is the ESA combined with the KMM.

the error is the average error of the function. These values are derived from the average of ten time tests.

$$f=\sum_{k=1}^{N_p}\frac{b_k}{1+\frac{(x-x_{pk})^2+(y-y_{pk})^2}{a_k}},\ (-50\le x,y\le 50) \quad (11)$$

5.3 Multi-Step optimization

The first optimization step is the optimization of the permanent magnet, the mover, and the stationary iron core through a magneto-static field analysis using the FEM to satisfy the required closing holding force. The variables are X_1 and X_2 as shown in Fig. 5.

For the opening holding force, the middle magnet can be designed prior to the optimization process because the opening holding force is generated only by the middle magnet and because the saturation does not occur by the middle magnet. The width of the permanent magnet, which has no effect on the magnetic flux density, is determined to be the minimum size, 8(mm), considering the demagnetization.

The closing coil also can be designed prior to the optimization process because saturation does not arise by the closing coil and because a high voltage drop of the closing capacitor is permitted due to its one time operation during the operating duty test, which is the estimation of the malfunction by carrying out the continuous operation of the closing and the opening. The operating duty test of the 17.5(kV)/40(kA) VCB involved an open-close-open sequence.

The variable ranges are as follows: $15<X_1<25$, $30<X_2<40$ (mm). The objective function is suggested by (12) using the multi-objective function. The first term on the right side of (12) serves to minimize the length of the permanent magnet. The second term is derived to ensure a close match

between the holding force and the required holding force of 7100(N) because the large holding force acts as a load during the opening process.

$$f_1 = \begin{cases} \dfrac{25 - X_1}{10} + \exp\left(-\dfrac{|F_{mag} - 7100|}{200} \right), & if\ F_{mag} > 7100 \\ 0 & ,othewise \end{cases} \quad (12)$$

The second optimization step involves the optimization of the opening coil to meet the requirements of the velocity of the movable electrode and the voltage drop of the opening capacitor. The horizontal length of the opening coil, X_3, should be shorter than the vertical length because if the horizontal length is longer than the vertical length, the end-winding effect is increased, inducing an increase in the inductance. Hence, the vertical length is determined to 1.5 times the size of the horizontal length. The variables for the second optimization step are the horizontal length, X_3, and the diameter of the opening coil, X_4. The variable ranges are as follows: $18<X_3<30$, $1.3<X_4<2$ (mm). The number of turns is determined automatically through the optimization process. The multi-objective function for the second optimization step is proposed by (13), where *vel* is the opening velocity and *RV* is the remaining voltage of the opening capacitor after completing the opening process.

$$f_2 = \frac{vel - 0.9}{1} + \frac{RV - 55}{30} \quad (13)$$

If the optimization for the SPMA is carried out by considering all variables together in an optimization process, both the magneto-static field and the dynamic characteristic have to be calculated for a model, of which dynamic characteristic analysis needs not to be calculated when the requirement of holding force is not satisfied through the magneto-static field analysis. In other words, much time is wasted by calculating the dynamic characteristic analysis using the time difference method for a useless model. In the proposed multi-step optimization method, the magneto-static field and the dynamic characteristics are analyzed in turn during the optimization of the independent variables.

Most of all, if the multi-step optimization is not used for the SPMA, the optima could not be found out without the convergence or much time is required for the convergence due to many variables. Hence, the optimization time can be reduced remarkably using the proposed multi-step optimization method.

5.4 Optimization result

As shown in Fig. 9, the length of the permanent magnet X_1 and the width of the mover X_2 are optimized to 19(mm) and 34(mm), respectively, satisfying the required closing holding force of 7116(N) after 346 function calls, which is

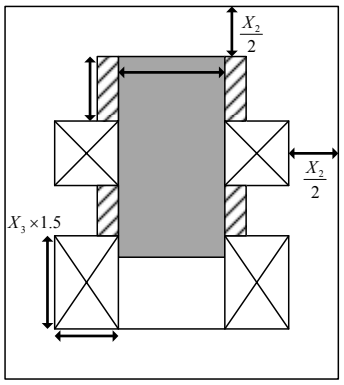

Fig. 8 Variables of the SPMA for the multi-step optimization.

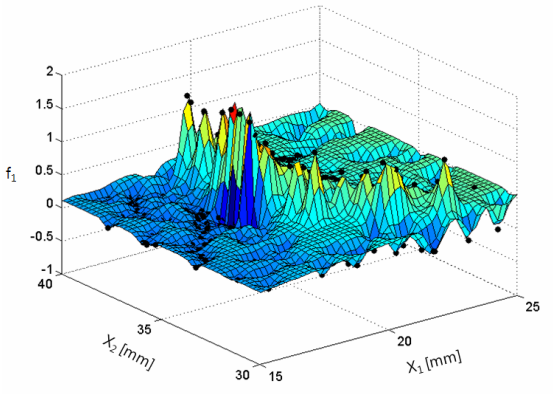

Fig. 9. The final KMM of the first optimization step

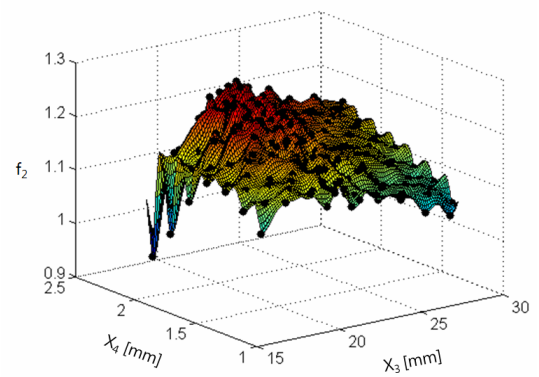

Fig. 10. The final KMM of the second optimization step

the number of samples, during the first optimization step. As tabulated in Table 1, the length of the permanent magnet of the optimized model was decreased by 10% from that of a basic model which is designed via analysis of dozens models by an expert designer for SPMA. This design process of the basic model is termed as the trial-and-error method in this research.

The width of the slot X_3 and the diameter of the opening coil X_4 are converged to 23.2(mm) and 2.1(mm), respectively, after 458 function calls during the second optimization step, as displayed in Fig. 10. The voltage drop

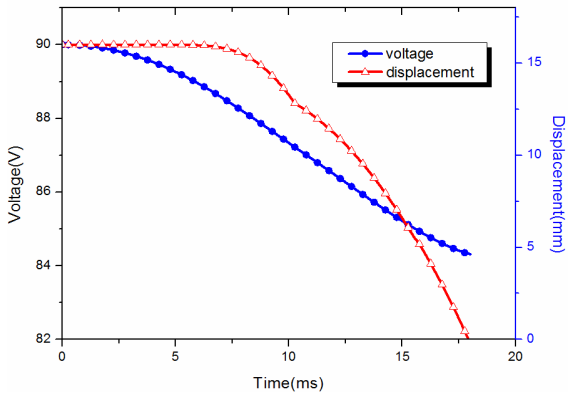

Fig. 11. The displacement of the movable electrode and the voltage of the opening capacitor during the opening operation of the optimized model

Table 1. Comparison between the basic model which was designed using the trial-and-error method and the optimized model

Specification	Basic model	Optimized model
Length of the permanent magnet(mm)	37.5	34
Number of turns of the opening coil	156	182
Resistance of the opening coil(Ω)	0.396	0.433
Opening velocity(m/s)	1.23	1.26
Voltage drop of opening capacitor(V)	10.8	5.7

of the opening capacitor in the optimized model was largely diminished, increasing the stability during the operating duty test compared to that of the basic model, as shown in Table 1.

Fig. 11 shows that the optimized SPMA satisfies all of the requirements. The opening velocity exceeded 1.2(m/s), which can prevent a dielectric breakdown. The voltage drop was under 10(V) for the operating duty test.

5. Conclusion

The remarkable finding in this paper is that for the novel PMA, which is termed the SPMA, the problems associated with the conventional trial-and-error design were solved. A fast and reliable optimal design was made possible through the proposed optimal design method which uses the characteristic analysis method, the multi-step optimization method, the ESA, and the KMM. The amount of the permanent magnet and the voltage drop of the opening capacitor were reduced compared to the basic model, leading to a decrease in the cost and an increase in the stability through rapid optimization using the proposed optimal design method. Hence, this research has significant meaning in that the proposed SPMA and the optimal design method can lead to the proliferation of a permanent magnetic actuator for CBs.

Acknowledgements

This Research was funded by Engineering Research Institute of Seoul National University.

References

[1] www.abb.com/mediumvoltage, "R-MAGTM magnetically actuated dead tank outdoor vacuum circuit breaker 15.5kV-38Kv," *1VAL255101-DB* March 2010.

[2] E. Dullni, H. Fink, C. Reuber, "A vaccum circuit-breaker with permanent magnetic actuator and electronic control," *http://www05.abb.com/global/scot/scot235.nsf /veritydisplay/ 5e750b2ecc5b760ec1256ad4002d2c00/$file/cired99_nice_vm1.pdf.*

[3] S. Fang, H. Lin, and S. L. Ho, "Transient co-simulation of low voltage circuit breaker with permanent magnet actuator," *IEEE Trans. Magn.,* vol. 45, no. 3, March, 2009.

[4] S. H. Lim and S. J. Min, "Design optimization of permanent magnet actuator using multi-phase level-set model," *IEEE Trans. Magn.,* vol. 48, no. 4, April, 2012.

[5] E. Dullni, "A vacuum circuit breaker with permanent magnetic actuator for frequency operations", *in Proc. of IEEE 18th International Symposium on Discharges and Electrical Insulation in Vacuum*, pp. 688-691, 1998.

[6] E. Dullni, H. Fink, M. Heimbach, and C. Reuber, "A family of vacuum circuit-breakers with worldwide applications using common components," *in CIRED 2001, 16th International Conference and Exhibition*, Conference Publication, no. 482, 2001.

[7] www.abb.com, "AMVACTM technical guide vacuum circuit breaker with magnetic actuator mechanism," *Technical guide AMVAC circuit breaker, 1VAF050601 -TG Rev H (replaces TG-IBAM-01),* January, 2010.

[8] B. A. R. Mckean and C. Reuber, "Magnets &Vacuum – The perfect match," *in proceedings 1998 IEE Trends in Distribution Switchgear*, London, pp.73-79, 1998.

[9] A. L. J. Janssen, "Final report of the second international enquiry on high voltage circuit breaker failures and defects in service," *CIGRE report,* no. 83, 1994.

[10] www.abb.com, "Installation and service instructions ANSI: 15 kV; 1200 A; 31.5 kA," *Instruction booklet*, April, 2011.

[11] Z. Cai, S. Ma, and J. Wang, "An approach of improve permanent magnetic actuator of vacuum circuit breaker," *XXIII-rd Int. Symp. on Discharges and Electrical Insulation in Vacuum – Bucharest–*, 2008.

[12] S. M. Lee, J. H. Kang, S. Y. Kwak, R. E. Kim, and H. K. Jung, "Dynamic characteristic analysis of electric

actuator for 1kV/3.2 kA air circuit breaker based on the three-link structure," *Journal of Electrical Engineering & Technology*, vol. 6, no. 5, pp. 613-617, September, 2011.
[13] S. K. Hong, D. K. Woo, and H. K. Jung, "Design of electromagnetic force driving actuator for automatic transfer breaker based on three-link structure," *International Conference on Electrical Machines and Systems (ICEMS)*, pp. 1-4, 20-23, August, 2011.
[14] A. Morita, M. Yabu, and K. Tsuchiya, "Vacuum circuit breaker with a new electromagnetic actuator," *International Conference on Electrical Engineering*, pp. 829, 2004.
[15] C. Hou, J. Sun, Y. Cao, X. Liu, and E. Wang, "Design and analyses on permanent magnet actuator for mining vacuum circuit breaker," *XXIInd Int. Symp. on Discharges and Electrical Insulation in Vacuum-Matsue-*, 2006.
[16] A. Goto, T. Okamoto, A. Ikariga, T. Todaka, and M. Enokizono, "A new moving-magnet type linear actuator utilizing flux concentration permanent magnet arrangement," *Journal of Electrical Engin-eering & Technology,* vol. 7, no. 3, pp. 342~348, 2012.
[17] J. H. Seo and H. K. Jung, "Optimal design of an IPMSM for high-speed operation using electro-magnetic and stress analysis," *Journal of Electrical Engineering & Technology,* vol. 4, no. 3, pp. 377~381, 2009.
[18] H. C. Jung, C. G. Lee, S. C. Hahn and S. Y. Jung, "Optimal design of a direct-driven PM wind generator aimed at maximum AEP using coupled FEA and parallel computing GA," *Journal of Elec-trical Engineering & Technology*, vol. 3, no. 4, pp. 552~558, 2008.
[19] L. Lebensztajn, C. A. R. Marretto, M. C. Costa, and J. L. Coulomb, "Kriging: A useful tool for electro-magnetic device optimization," *IEEE Trans. Magn.,* vol. 40, no. 2, March, 2004.
[20] M. Shaohua, W. Jimei, "Research and design of permanent magnetic actuator for high voltage vacuum circuit breaker", *International Symposium on Discharges and Electrical Insulation in Vacuum*, pp. 487-490, 2002.
[21] D. K. Cheng, Field and Wave Electromagnetics, *2nd edition, Addison-Wesley : New York*, 1992.
[22] B. Lequesne, "Fast-acting long-stroke bistable solenoids with moving permanent magnets," *IEEE Trans. Ind. Appl.*, vol. 26, no. 3, pp. 574 - 581, 1990.
[23] T. Bäck, "Evolutionary algorithms in theory and practice", Oxford, U.K.: Oxford Univ. Press, 1996.
[24] J. S. Rho, C. H. Lee, H. K. Jung, "Optimal design of ultrasonic motor using evolution strategy and finite element method", International Journal of Applied Electromagnetics and Mechanics, vol. 25, no. 1, pp. 699-704, July, 2007.
[25] K. H. Chong, I. B. Aris, S. M. Bashi and S. P. Koh, "Design of digital circuit structure based on evolutionary algorithm method," *Journal of Electrical Engineering & Technology*, vol. 3, no. 1, pp. 43~51, 2008.

SeungKi Hong received his B.S. degree in Electrical Engineering from Inha University, Incheon, Korea, in 2009. He received his M.S. degree in Electrical Engineering from Seoul National University, Seoul, Korea, in 2012. He is currently an assistant research engineer in LSIS. Co. Ltd. His research is focused on the analysis and design of the actuator for circuit breakers.

Jong-Suk Ro received the B.S. degree in Mechanical Engineering from Han-Yang University, Seoul, Korea, in 2001. In 2008, he earned a PhD in Electrical engineering from Seoul National University, Seoul, Korea, through the Combined Master's and Doctorate Program. He conducted research at R&D center of Samsung Electronics as a Senior Engineer from 2008 to 2012. From 2012 to 2013, he was at Brain Korea 21 Information Technology of Seoul National University as a Post-Doctoral Fellow. He carried out research at Electrical Energy Conversion System Research Division of Smart Grid Team at Korea Electrical Engineering & Science Research Institute as a Researcher in 2013. Currently, he is at Brain Korea 21 Plus, Creative Research Engineer Development, Department of Electrical and Computer Engineering, Seoul National University as a BK Assistant Professor. His research interest is characteristic analysis and design of energy conversion devices

Hyun Kyo Jung (S'82-M'90-SM'99) received the B.S., M.S., and Ph.D. degree in Electrical engineering from the Seoul National University, Seoul, Korea, in 1979, 1981, and 1984, respectively. From 1985 to 1994, he was a member of the faculty with Kangwon National University. From 1987 to 1989, he was with the Polytechnic University of Brooklyn, Brooklyn, NY. From 1999 to 2000, he was a Visiting Professor with the University of California at Berkeley. He is currently a Professor at the School of Electrical Engineering and Computer Science/Electrical Engineering, Seoul National University. His research interests are the analysis and design of the electric machine.